Journal of Alloys and Compounds 513 (2012) 101–106

Contents lists available at SciVerse ScienceDirect

Journal of Alloys and Compounds

journal homepage: www.elsevier.com/locate/jallcom

Normal spectral emittance of Inconel 718 aeronautical alloy coated with yttria stabilized zirconia films

L. González-Fernández[a,b], L. del Campo[a,1], R.B. Pérez-Sáez[a,*], M.J. Tello[a]

[a] Departamento de Física de la Materia Condensada, Facultad de Ciencia y Tecnología, Universidad del País Vasco, Barrio Sarriena s/n, 48940 Leioa, Bizkaia, Spain
[b] Industria de Turbo Propulsores, S.A., Planta de Zamudio, Edificio 300, 48170 Zamudio, Bizkaia, Spain

ARTICLE INFO

Article history:
Received 29 July 2011
Received in revised form
28 September 2011
Accepted 30 September 2011
Available online 8 October 2011

Keywords:
Coating materials
High-temperature alloys
Optical properties
Infrared spectroscopy

ABSTRACT

Knowledge of the radiative behaviour of the yttria stabilized zirconia (YSZ) thermal barrier coatings (TBCs) is needed to perform radiative heat transfer calculations in industrial applications. In this paper, normal spectral emittance experimental data of atmospheric plasma sprayed (PS) YSZ films layered on Inconel 718 substrates are shown. The spectral emittance was measured between 2.5 and 22 μm on samples with film thicknesses ranging from 20 to 280 μm. The samples were heated in a controlled environment, and the emittance was measured for several temperatures between 330 and 730 °C. The dependence of the spectral emittance with film thickness, surface roughness and temperature has been studied and compared with the available results for YSZ TBCs obtained by electron-beam physical vapour deposition. The PS-TBC samples show a Christiansen point at $\lambda = 12.8$ μm. The films are semi-transparent for $\lambda < 9$ μm, and opaque for $\lambda > 9$ μm. In the semi-transparent region, the contribution of the radiation emitted by the Inconel 718 substrate to the global emittance of the samples is analysed. In addition, the influence of the roughness in the emittance values in the opaque spectral region is discussed. Finally, the total normal emittance is obtained as a function of the TBC thickness.

1. Introduction

Zirconia (ZrO_2) is widely used in several technological and industrial applications due to its refractory and corrosion resistance properties. This compound is usually mixed with other oxides, such as yttria (Y_2O_3), which can partially or thoroughly stabilize the high temperature cubic phase down to ambient temperature [1], and improve the thermal and mechanical performance of the undoped zirconia. In addition to the above-mentioned properties, zirconia has a very low thermal conductivity and it is a good reflector of radiant heat flux. Both properties are very useful in heat barrier systems. Thus, yttria stabilized zirconia (YSZ) thermal barrier coating (TBC) systems produced by plasma spraying (PS) or electron-beam physical vapour deposition (EB-PVD) on metallic substrates is extensively employed in order to reduce the heat load in, for example, turbine engines [2–5]. TBCs are able to support high temperature gradients between the side exposed to severe temperatures and the metallic substrate, which has to be maintained at much lower temperature. In addition, it protects the metal from corrosion [6].

The aeronautical industry is directly related to the use and development of these TBCs, but they are also of special interest to aerospace, computer and optical engineerings. Gas turbine, solar energy and thermophotovoltaic radiator applications are also concerned with YSZ coatings [2,7,8]. In all these applications, it is very important to account for the radiative behaviour of the system. The emissivity of a radiating surface is a necessary parameter when performing thermal radiation heat transfer calculations [3,9]. In addition, the knowledge of the emissivity of a surface allows the pyrometric (radiometric) measurement of its temperature [10].

Some studies on the radiative properties of YSZ thermal barrier coatings are found in the literature [2–8,11,12]. The measurements on plasma-sprayed thermal barrier coatings (PS-TBCs) [2] and on EB-PVD thermal barrier coatings (EB-PVD-TBCs) [3,4] show that the YSZ TBC is spectrally selective, and the emissivity decreases as the ceramic coating thickness increases. This is due to the semi-transparency of the YSZ coating, and the experimental results account for an apparent emittance of the TBC/substrate system. However, the EB-PVD-TBCs seem to be opaque for ceramic thicknesses higher than 150 μm [3], while the PS-TBCs are still semi-transparent for coatings 330 μm thick [2]. Additionally, absorption peaks due to adsorbed water and carbon dioxide were clearly detected in EB-PVD-TBCs, while they do not appear in PS-TBCs [2,3]. Thus, the characteristics of the coatings prepared by these two techniques (PS and EB-PVD) seem to differ substantially. For PS-TBCs, it was found that the normal and

* Corresponding author. Tel.: +34 94 601 2655; fax: +34 94 601 3500.
E-mail address: raul.perez@ehu.es (R.B. Pérez-Sáez).
[1] Present address: Departamento de Física Aplicada II, Facultad de Ciencia y Tecnología, Universidad del País Vasco, Barrio Sarriena s/n, 48940 Leioa, Bizkaia, Spain.

0925-8388/$ – see front matter © 2011 Elsevier B.V. All rights reserved.
doi:10.1016/j.jallcom.2011.09.097

hemispherical spectral emittance did not change between 300 and 1590 K, and it was also stated that this property did not change with the surface roughness and emission angle [2]. For YSZ thermal barrier coatings prepared by EB-PVD, the dependence of the emissivity on wavelength, emission angle, temperature and layer thickness was studied in Ref. [3], and it was found that for coating thicknesses higher than 150 μm the emissivity is nearly constant. Experimental data of spectral directional-hemispherical reflectance and transmittance for plasma sprayed YSZ samples with thicknesses above 320 μm were also published [11]. However, only ambient temperature was considered. Total hemispherical emittance for these thermal barrier coatings has also been reported [7], as well as studies at short wavelength (visible and near infrared) [12].

As explained in Ref. [3], YSZ TBCs prepared by EB-PVD seem to have some advantageous features when applied to movable parts of gas turbine engines. On the other hand, laser melting of the coating might be used to improve the tightness, hardness and erosion resistance of the PS-TBCs [13]. Thus, additional emissivity measurements on PS-TBCs are needed in order to carry out a comparison of the radiative behaviour of TBCs produced using PS and EB-PVD. With the aim to advance in this characterization, the spectral emittance of atmospheric plasma sprayed YSZ films on Inconel 718 aeronautical alloys with several film thicknesses and surface roughness is measured and analysed in this paper. The measurements were performed using a high accuracy infrared radiometer (HAIR) with technical parameters close to the ones used for the measurement of the emissivity on YSZ thermal barrier coatings prepared by EB-PVD [3]. In Section 2, the samples studied are described, and the experimental procedure is explained. In Section 3, the experimentally obtained spectral emittance is shown as a function of wavelength and temperature (Section 3.1), as a function of the thermal cycle (Section 3.2), and as a function of the film thickness and surface roughness (Section 3.3). Results in Section 3 are discussed in Section 4, and a qualitative explanation of the radiative behaviour of YSZ thermal barrier coatings is given. Finally, in Section 5 some conclusions are argued.

2. Experimental

2.1. Samples

Inconel 718 samples coated with atmospheric plasma sprayed yttria (8 wt%) stabilized zirconia (YSZ) have been studied in this paper. The atmospheric plasma spraying process for thermal barrier coating preparation is very well described in the literature [2,14]. The chemical composition of Inconel 718 (substrate), in weight percentage, is shown in Table 1. Substrates with disc form and thickness of 3 mm were wire-cut from a 60 mm diameter rod using an electrical discharge machine (EDM). The surfaces of the substrates were sandblasted in order to remove the recast layer due to the machining cut. The sandblasting also increases the roughness of the substrate, which enhances the mechanical anchorage between the substrate and the ceramic layer, avoiding the use of a bond-coat for small layer thicknesses. A bond-coat of nickel and aluminium was applied in the three samples with the thickest coatings (samples 7–9 in Table 2). After applying the YSZ coating, the surfaces of the samples were ground to obtain the desired roughness.

Eight samples with different ceramic thickness and surface roughness have been prepared, to analyse the influence of these physical parameters in the spectral emittance. A sandblasted but uncoated sample (sample 1) has also been prepared to study the substrate emissivity and its influence in the global emittance. Table 2 shows the thickness and some roughness data of the nine samples studied: the surface roughness average (R_a), average maximum height (R_z) and maximum height of the profile (R_t). The coating thickness has been measured with a Dualscope FMP20 equipped with an FTA3.3 probe, and the roughness measurements have been carried out with a Mitutoyo SJ201 in two perpendicular directions in order to detect anisotropies on the samples. SEM images (Fig. 1) were obtained in order to characterize the microstructure of the coatings. Micrographs obtained for sample 5 (see Fig. 1) are similar to those found in the literature (Fig. 1 of Ref. [2]).

Table 1
Chemical composition of Inconel 718 in weight percentage.

Al	B	C	Co	Cr	Cu	Fe	Mn
0.2–0.8	Max. 0.006	Max. 0.08	Max. 1	17–21	Max. 0.3	Balance (~20)	Max. 0.35

Mo	Nb	Ni	P	S	Si	Ti
2.8–3.3	4.75–5.5	50–55	Max. 0.015	Max. 0.015	Max. 0.35	0.65–1.15

Table 2
Summary of the samples with their coating thickness and surface roughness: average roughness (R_a), average maximum height (R_z) and maximum height of the profile (R_t).

Sample	Coating	Thickness (μm)	R_a (μm)	R_z (μm)	R_t (μm)
1	Uncoated	–	7.55	51.99	64.36
2	ZrO_2 + 8 wt% yttria	18	2.14	26.06	31.06
3	ZrO_2 + 8 wt% yttria	24	8.70	57.28	66.87
4	ZrO_2 + 8 wt% yttria	34	3.42	22.64	27.88
5	ZrO_2 + 8 wt% yttria	38	2.09	16.16	20.40
6	ZrO_2 + 8 wt% yttria	64	2.22	16.47	21.26
7	ZrO_2 + 8 wt% yttria	207	1.86	18.15	25.23
8	ZrO_2 + 8 wt% yttria	246	4.66	36.47	48.63
9	ZrO_2 + 8 wt% yttria	279	10.43	66.81	84.06

2.2. Emittance measurements

The emittance measurement of samples has been carried out with a high accuracy homemade infrared radiometer (HAIR) [15] in a spectral range between 2.5 and 22 μm, and a temperature range between 330 and 730 °C. The sample chamber allows to control the environment of the samples, thus, after performing a preliminary vacuum, a slightly reducing gas (N_2 + 5%H_2) was used in order to minimize the presence of oxygen during the measurements of emissivity. Axial temperature gradients are expected, which have to be considered in the region where the samples are semi-transparent. In order to optimize the temperature measurement of the YSZ layer, it is calculated by means of a combination of two methods: on the one hand, two bare K-type thermocouples are spot welded to the substrate removing the coating film, out of the area viewed by the detector; on the other hand, the Christiansen point of the ceramic layer where the sample behaves like a blackbody is used to correct the temperature so as to set $\varepsilon = 1$ at that point [16,17], which is located at $\lambda = 12.8$ μm in the YSZ radiative spectra.

Taking into account previous studies about the accuracy of the measurement methods [18], the normal spectral emittance (ε) is obtained using the so-called blacksur method, which accounts not only for emitted radiation, but also for the radiation of the surroundings reflected by the sample. Thus, the radiation leaving the sample (L_s^*) can be written as

$$L_s^* = \varepsilon L_s + (1-\varepsilon)L_{sur}, \tag{1}$$

where the subscripts *s* and *sur* refer to the sample and the surroundings, respectively, while L_i is the spectral directional emission intensity given by Planck's equation at temperature T_i. From Eq. (1), the emittance can be obtained as

$$\varepsilon = \frac{L_s^* - L_{sur}}{L_s - L_{sur}}. \tag{2}$$

In order to determine the emittance applying Eq. (2), it is necessary to measure the radiation coming from the sample, which is affected by the response function (R) and the offset radiation (S_0) of the spectrometer in the following way [19]:

$$S_s = RL_s^* + S_0, \tag{3}$$

where S_s is the sample radiation measured by the radiometer. Therefore, a calibration of the device must be carried out to determine R and S_0. Taking into account previous analysis of the calibration and uncertainties of the measurements [19,20], a modified two-temperature method is used to calibrate the radiometer. In this method, signals of a blackbody and a greybody of known emissivity are required; the signal of the greybody is obtained with a shutter coated with Nextel Velvet Coating 811-21 [21], which is placed in front of the blackbody radiator. Thus, R and S_0 are calculated as

$$R = \frac{S_{bb} - S_{gr}}{L_{bb} - \varepsilon_{gr}L_{gr}}, \qquad S_0 = S_{bb} - RL_{bb} = S_{gr} - R\varepsilon_{gr}L_{gr}. \tag{4}$$

Combining the abovementioned equations, the normal spectral emittance is obtained according to the following expression:

$$\varepsilon = \frac{\mathrm{FT}(I_s - I_{gr})}{\mathrm{FT}(I_{bb} - I_{gr})} \times \frac{L_{bb} - \varepsilon_{gr}L_{gr}}{L_s - L_{sur}} + \frac{\varepsilon_{gr}L_{gr} - L_{sur}}{L_s - L_{sur}}, \tag{5}$$

where the subscripts *s*, *bb*, *gr* and *sur* stand for sample, blackbody, grey body and sample surroundings, respectively. FT represents Fourier transform, and I_i the interferogram. It has to be noted that when measuring with an FT-IR spectrometer it is advisable to subtract the interferograms before Fourier transforming, rather than subtracting transformed signals thus S_s–S_{gr} and S_{bb}–S_{gr} are replaced by FT(I_s–I_{gr}) and FT(I_{bb}–I_{gr}), respectively. The measurement method in this paper differs from

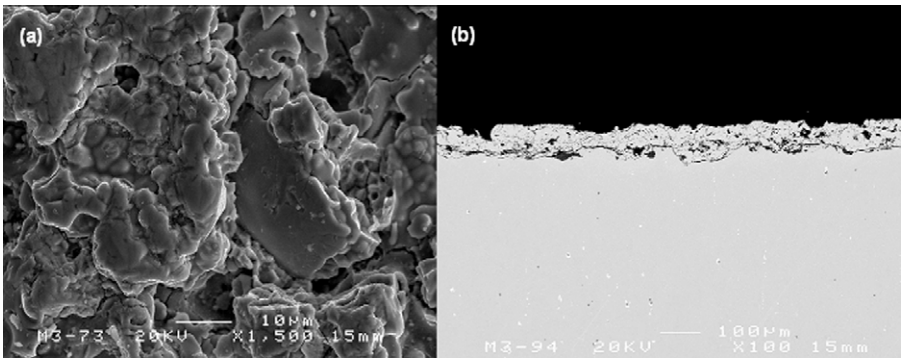

Fig. 1. SEM images of sample 5 (38 μm coating): (a) surface and (b) cross-section.

the one used in the literature to obtain the spectral radiation properties of YSZ thermal barriers coatings prepared by PS [2]. This point, together with the atmosphere control, is an important factor determining the results.

For each sample, two thermal cycles have been carried out between room temperature and 730 °C. The emittance spectra have been measured with temperature intervals of 100 °C during the two heating cycles, and the samples were cooled down to room temperature after each of them. The aim of this process is to check the effect of the thermal history on the emittance values.

3. Results

In this section the experimental results obtained for the dependence of the emissivity on wavelength, temperature, thermal cycling, film thickness and roughness are shown.

3.1. Temperature and wavelength dependence

In Fig. 2, the spectral normal emittance of sample 5 (38 μm coating) obtained during the first heating cycle is shown as a function of the wavelength for several temperatures. The presence of a large emittance plateau with values close to one between 9 and 14 μm is remarkable. The experimentally found Christiansen point is located at λ = 12.5–12.8 μm, in good agreement with the value λ = 13 μm found in the literature for EB-PVD-TBCs [3]. In the results for PS-TBCs shown in Ref. [2], the Christiansen point is difficult to identify. The difference between the plateau in Fig. 5 of Ref. [3] and that in Fig. 2 of this paper is due to the film thickness. For wavelengths longer than the Christiansen point, the emittance increases with the sample temperature, but the dependence is not very strong, with an increase of the emittance lower than 10% between 328 °C and 708 °C. The same behaviour is observed in EB-PVD-TBCs [3]. In the short wavelength region only the 708 °C spectrum differs from the general tendency, which means that a change takes place in the sample at highest temperature during the first heating cycle. As it can be noticed, there are some peaks in spectra at short wavelengths. The peaks around λ = 6.5 μm and λ = 2.9 μm are due to the vibrations of the OH group of the H_2O molecule and the peak around λ = 4.3 μm corresponds to the CO bond of the CO_2 molecules trapped on the coating during the plasma spray process. These peaks were found in EB-PVD-TBCs but they were not seen in PS-TBCs [2,3].

3.2. Thermal history dependence

Fig. 2 shows an emittance increase at short wavelengths and high temperature (708 °C) which could be produced by the substrate because, as already mentioned in the introduction, the TBC is semi-transparent in this spectral range. In order to look for the cause of this anomalous behaviour, the spectral normal emittance of sample 5 (38 μm coating) obtained during the first and the second heating cycles are plotted in Fig. 3 as a function of the wavelength for two different temperatures. As it is shown, in both cases there is no change in the spectrum between the first and the second heating cycle for wavelengths longer than 7 μm. For short wavelengths, almost no difference is found for the highest temperature (710 °C), while for the lowest temperature (520 °C) the emittance increases from the first to the second cycle; this behaviour occurs in all the studied samples. This fact suggests that this effect is due to a change in the emissive properties of the samples that takes place during the first heating cycle between 600 °C and 700 °C and becomes permanent.

To check the substrate effect, the same measurement process has been carried out on an uncoated sandblasted Inconel 718 (sample 1). The spectral normal emittance during two heating cycles on sample 1 measured at 550 °C is shown in Fig. 4. The same effect that appears for the PS-TBC in Fig. 3 is observed for short wavelengths. Dependence of the emissivity with the thermal history was already observed in other metals and alloys [22–24].

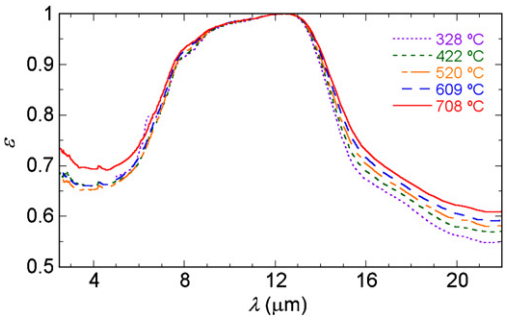

Fig. 2. Spectral normal emittance of sample 5 (38 μm coating) as a function of the wavelength for several temperatures, measured during the 1st heating cycle.

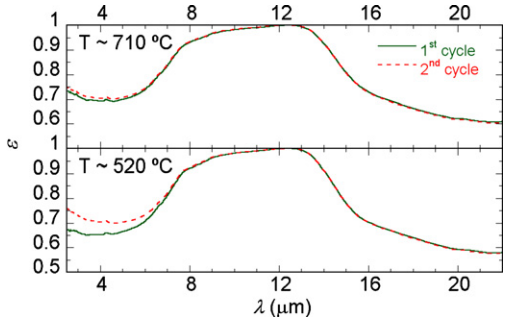

Fig. 3. Spectral normal emittance of sample 5 (38 μm coating) as a function of the wavelength at $T \sim 520$ and $T \sim 710$ °C during the 1st and 2nd heating cycles.

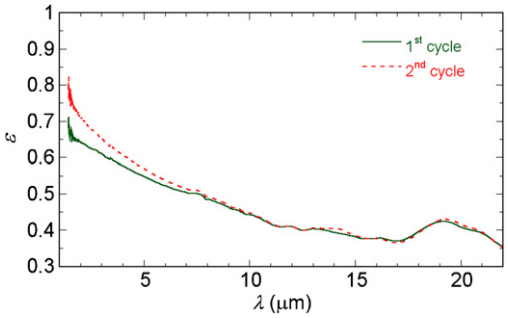

Fig. 4. Spectral normal emittance of sample 1 (uncoated) as a function of the wavelength at $T \sim 550\,^{\circ}C$ during the 1st and 2nd heating cycles.

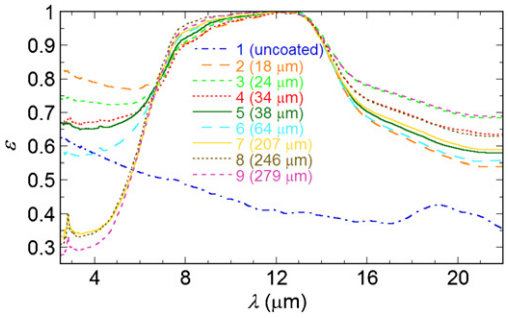

Fig. 5. Spectral normal emittance of YSZ TBCs and the bare substrate as a function of the wavelength at $T \sim 520\,^{\circ}C$ obtained during the 1st heating cycle.

3.3. Film thickness and surface roughness

Following, the influence of the thickness of the TBC on the emissivity has been taken into consideration. In Fig. 5, the spectral normal emittance for all the coated samples and the bare substrate measured during the first heating cycle at a temperature of around 520 °C has been plotted as a function of the wavelength. On the one hand, as expected, the experimental results show a Christiansen point for all the coated samples at the same wavelength. On the other hand, the experimental values of the emittance show a considerable dispersion among spectra for both, short and long wavelengths. As it will be explained in next section, the cause of the dispersion at short wavelengths is not the same as that for long wavelengths. It should also be noted that the width of the platform that contains the Christiansen point enlarges with the TBC thickness.

The spectral normal emittance of the coated samples as a function of the YSZ layer thickness and measured at a temperature around 520 °C has been represented for several wavelengths below the Christiansen point in Fig. 6. The experimental plots in Fig. 6 show that for wavelengths shorter than 7 μm the

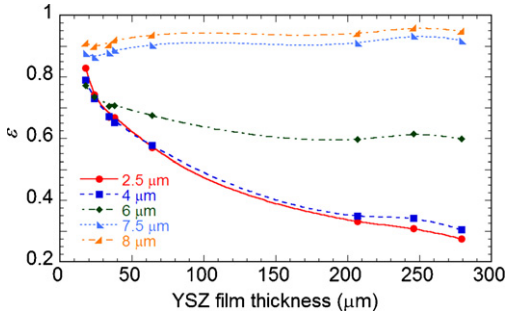

Fig. 6. Spectral normal emittance of YSZ TBCs as a function of the film thickness at $T \sim 520\,^{\circ}C$ for several wavelengths obtained during the 1st heating cycle.

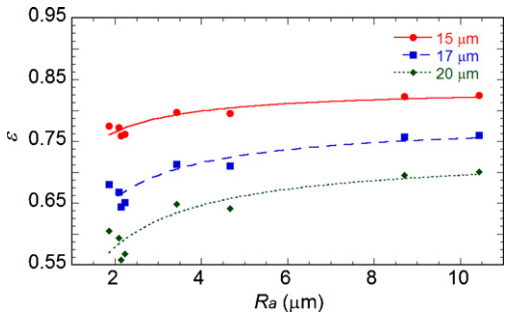

Fig. 7. Spectral normal emittance of YSZ TBCs as a function of surface roughness at $T \sim 520\,^{\circ}C$ for three different wavelengths obtained during the 1st heating cycle.

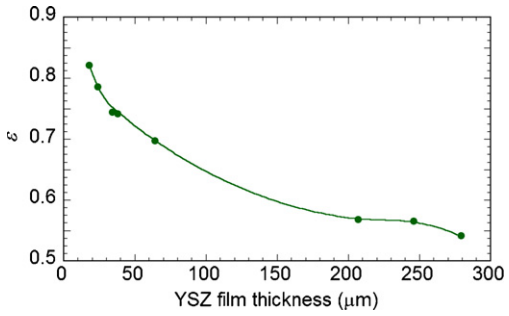

Fig. 8. Spectrally integrated emittance of YSZ TBCs as a function of the film thickness at $T \sim 520\,^{\circ}C$ obtained during the 1st heating cycle.

emittance decreases as the YSZ coating thickness increases. However, for wavelengths between 7 μm and the Christiansen point ($\lambda \approx 12.8$ μm) this behaviour is reversed, and the emittance value slightly increases as the thickness rises.

In order to check the effect of the roughness on the radiative behaviour, the spectral normal emittance of the coated samples determined at a temperature around 520 °C has been represented in Fig. 7 as a function of the average roughness for three different wavelengths above the Christiansen point. As observed, the emittance values increase as the roughness does.

So as to study the effect of film thickness on the global radiative behaviour of the YSZ PS-TBC, the emittance integrated between $\lambda = 1.43$ μm and $\lambda = 25$ μm has been calculated at $T \sim 520\,^{\circ}C$ for all the samples described in Table 2, and whose spectral normal emittance has been plotted in Fig. 5. This spectrally integrated emittance accounts for more than 98% of the total emittance. The results are shown in Fig. 8, as a function of the film thickness. As observed, the integrated emittance decreases with film thickness, due to the decrease of the spectral emittance at short wavelengths. This parameter has to be used when performing radiative heat transfer calculation since it accounts for the radiation actually emitted by the YSZ PS-TBC/Inconel 718 system.

4. Discussion

So as to understand and analyse the results shown in previous section, the opaque and semi-transparent spectral ranges for the YSZ films have to be identified. The long wavelength infrared response (higher wavelengths than the Christiansen point) is guided by the interaction between the electromagnetic radiation and the modes of vibration of the crystal structure. Due to interaction between phonons, the absorption is not only limited to the resonance frequencies and this entire spectral region is opaque. Decreasing the wavelength of the infrared light (lower wavelengths than the Christiansen point), the YSZ remains opaque until $\lambda \sim 9$ μm [4,25] (the exact value depends on the coating

thickness) due to multi-phonon absorption processes, and it becomes semi-transparent at lower wavelengths. We can find the transmission front in this semi-transparent region of the spectrum, which will also be settled by multi-phonon absorption processes.[2]

Therefore, for the TBCs studied in this paper, the measured emittance values have different origins above or below $\lambda = 9\ \mu m$. On the one hand, the emittance for $\lambda > 9\ \mu m$ is the emittance of the YSZ, that is, the substrate is not visible by infrared spectroscopy. The spectral radiative response will mainly vary with surface roughness. On the other hand, the emittance for $\lambda < 9\ \mu m$ is an apparent emittance which includes both the radiance of the YSZ film and that of the substrate. The spectral emittance will mainly be affected by film thickness. Figs. 5–7 show that the emittance increases with roughness for long wavelengths and decreases with film thickness for short wavelengths.

4.1. Semi-transparent spectral region ($\lambda < 9\ \mu m$)

The semi-transparency in this spectral region is due to the high transmittance of the film for these wavelengths. In the case of the YSZ films a transmittance maximum is found around 4–6 μm for both PS [11,26] and EB-PVD [3] coatings.

The analysis carried out provides evidence of the fact that the change in the emittance between the first and the second thermal heating cycles shown in Fig. 3 is directly related to a change in the radiative response of the substrate. This fact has been confirmed through a measurement performed on the substrate and shown in Fig. 4. Emissivity evolution with the temperature has already been observed in metallic samples in previous studies [22–24]. As suggested in Ref. [22], the emissivity increase of the bare Inconel 718 could be related to a slight oxidation of the metallic surface. This hypothesis is in agreement with the cracked and porous structure of the TBCs shown in Fig. 1b, which do not completely prevent the corrosion of the substrate.

It has also been confirmed that the PS-TBCs, like the EB-PDV-TBCs [3], contain H_2O and CO_2 molecules, which are trapped in the interstices of the coating during the fabrication processes (Figs. 2 and 5). Nevertheless, the intensity of the related absorption peaks suggests that the EB-PDV give rise to TBCs which are richer in these species than the PS process. These absorption peaks are not present in the second heating cycle of samples studied in this paper, thus, contrary to what happens in EB-PDV-TBCs [3], the desorption process is not reversible in PS-TBCs. Moreover, the absorption peaks due to H_2O and CO_2 molecules are more pronounced in the samples with the thickest coating (see Fig. 5).

To explain the dependence of the spectral normal emittance with the coating thickness in the semi-transparent spectral region (Fig. 5) it must be taken into account that it will depend on the emittance of both the substrate and the coating. Furthermore, it should be noted that axial gradients of temperature due to the below heating of the samples leads to higher values on the apparent emittance, because hotter parts of the TBCs are also contributing. As the ceramic film gets thicker, the transparency of the TBCs decreases. Thus, the substrate contribution becomes less important in the apparent emittance, and it tends to the emittance of the opaque YSZ. That is, the apparent emittance in the semi-transparent region is a combined and weighted contribution of the substrate and YSZ emittances with an additional contribution due to hotter inner parts (axial gradient of temperature), which enhances the value of the apparent emittance. As the curves of the substrate (curve no. 1 in Fig. 5) and YSZ (it should be very close to curve no. 9 in Fig. 5) cut each other, the evolution of the apparent emittance with the coating thickness should be different at each side of the cut. The effect of the temperature axial gradient shifts the behaviour change to longer wavelengths. So, it is observed that the apparent emittance decreases with the coating thickness for wavelengths shorter than 7 μm and it increases with thickness between 7 and 9 μm. Nevertheless, experimental results for samples 7 and 8 in Fig. 5 seem to contradict this general tendency below 7 μm, because considering the film thickness of both samples we would expect the emittance of sample 8 to be lower than the emittance of sample 7. However, this apparent anomalous result is explained by the roughness of these two samples, since the roughness values of the sample 8 are more than twice those of the sample 7.

It is interesting to remark that in the PS-TBCs analysed in this paper the coatings remain transparent at least until ~280 μm, since the emittance still decreases in the short wavelength range for thicknesses between 246 μm and 279 μm (see Fig. 5). Additionally, the emittance at short wavelength also increases at high temperatures for sample 9. For samples with coating thickness more than 280 μm, the emittance will still decrease until the coating is thick enough to be opaque in this spectral range. PS-TBCs analysed in Ref. [2] also remain transparent at least until ~330 μm, whereas samples with 510 μm of thickness are opaque. This is an important difference between the radiative behaviour of PS-TBCs and EB-PVD-TBCs, for which the opaque behaviour is achieved for coating thicknesses ~150 μm [3].

4.2. Opaque spectral region ($\lambda > 9\ \mu m$)

In the long wavelength region the emittance values are independent of the coating thickness and the dispersion in the emittance values observed in Fig. 5 is due to variation in the surface roughness of the coating. According to Fig. 7 the emittance increases with roughness. The small dispersion in the values of emittance for samples with similar roughness is in agreement with the experimental uncertainties. In addition, it must be noticed that the temperature of the experimental emittance spectra in Fig. 7 is not exactly the same for all the samples. This fact can also introduce small differences in the experimental values.

Additionally, it is interesting to remark that the evolution of the emittance with the temperature in this opaque region has a different origin than the evolution at short wavelengths, and it is a consequence of the change of the damping of the infrared active modes of the YSZ with the temperature.

5. Conclusions

In addition to the Christiansen point at $\lambda = 12.8\ \mu m$, where the samples behave as a blackbody, a high emittance plateau has been found in the Inconel 718 samples coated with YSZ, even for the thinnest layers. The width of the plateau increases with the TBCs thickness.

The TBCs studied in this paper show a semi-transparent region below 9 μm. Above this wavelength, the ceramic coating is opaque. In the semi-transparent spectral range the level of the emittance is determined by the thickness of the coating. The emittance decreases below 7 μm and increases from 7 to 9 μm with coating thickness. In the opaque spectral region the surface roughness guides the emittance, growing in the same direction.

The experimental results in this paper together with those published in Ref. [2] ensure that for $\lambda < 9\ \mu m$ the YSZ PS-TBCs are semi-transparent for coating thicknesses under ~300 μm, whereas the YSZ EB-PVD-TBCs achieve opacity for ~150 μm [3].

The difference between the semi-transparency limit as a function of the coating thickness, and the quantity of adsorbed H_2O and

[2] P. Echegut and D. De Sousa Meneses, CEMHTI-CNRS Orleans (France), Personal comunication.

CO_2 molecules are a proof of the differences in the microstructure of PS and EB-PVD yttria stabilized zirconia thermal barrier coatings.

Acknowledgements

This work has been carried out with the financial support of the SAIOTEK program (Project number S-PC08UN07) of the Basque Government and the "Universidad-Empresa" program (Project number UE06/01) of the University of the Basque Country in collaboration with "Industria de Turbo Propulsores S.A.". L. González-Fernández acknowledges the Basque Government and Industria de Turbo Populsores S.A. their support through a Ph.D. fellowship.

References

[1] S.A. Ostanin, E.I. Salamatov, Pis'ma v ZhETF 74 (2001) 625–629.
[2] C.H. Liebert, NASA Tech. Pap. 1190 (1978).
[3] J. Manara, R. Brandt, J. Kuhn, J. Fricke, T. Krell, U. Schulz, M. Peters, W.A. Kaysser, High Temp. High Press. 32 (2000) 361–368.
[4] J. Manara, M. Arduini-Schuster, H.-J. Rätzer-Scheibe, U. Schulz, Surf. Coat. Technol. 203 (2009) 1059–1068.
[5] A. Jadhav, N.P. Padture, F. Wu, E.H. Jordan, M. Gell, Mater. Sci. Eng. A 405 (2005) 313–320.
[6] A. Keyvani, M. Saremi, M. Heydarzadeh Sohi, J. Alloys Compd. 509 (2011) 8370–8377.
[7] A. Ferriere, L. Lestrade, J-F. Robert, Sol. Energy Eng. 122 (2000) 9–13.
[8] B.V. Cockeram, J.L. Hollenbeck, Surf. Coat. Technol. 157 (2002) 274–281.
[9] G. Lim, A. Kar, J. Mater. Sci. 44 (2009) 3589–3599.
[10] F.E. Pfefferkorn, F.P. Incropera, Y.C. Shin, J. Heat Transfer 125 (2003) 48–56.
[11] L.A. Dombrovsky, H.K. Tagne, D. Baillis, L. Gremillard, Infrared Phys. Technol. 51 (2007) 44–53.
[12] A.M. Limarga, D.R. Clarke, Int. J. Appl. Ceram. Technol. 6 (2009) 400–409.
[13] K. Kobylańska-Szkaradek, J. Alloys Compd. 505 (2010) 516–522.
[14] A. Mirahmadi, M. Pourmalek, Ionics 16 (2010) 447–453.
[15] L. del Campo, R.B. Pérez-Sáez, X. Esquisabel, I. Fernández, M.J. Tello, Rev. Sci. Instrum. 77 (2006) 113111.
[16] B. Rousseau, J.F. Brun, D. De Sousa Meneses, P. Echegut, Int. J. Thermophys. 26 (2005) 1277–1286.
[17] J. Manara, M. Arduini-Schuster, M. Keller, Infrared Phys. Technol. 54 (2011) 395–442.
[18] R.B. Pérez-Sáez, L. del Campo, M.J. Tello, Int. J. Thermophys. 29 (2008) 1141–1155.
[19] L. González-Fernández, R.B. Pérez-Sáez, L. del Campo, M.J. Tello, Appl. Opt. 49 (2010) 2728–2735.
[20] L. del Campo, R.B. Pérez-Sáez, L. González-Fernández, M.J. Tello, J. Appl. Phys. 107 (2010) 113510.
[21] E.T. Kwor, S. Matteï, High Temp. High Press. 33 (2001) 551–556.
[22] L. del Campo, R.B. Pérez-Sáez, L. González-Fernández, X. Esquisabel, I. Fernández, P. González-Martín, M.J. Tello, J. Alloys Compd. 489 (2010) 482–487.
[23] L. del Campo, R.B. Pérez-Sáez, M.J. Tello, X. Esquisabel, I. Fernández, Int. J. Thermophys. 27 (2006) 1160–1172.
[24] E. Risueño, L. González-Fernández, R.B. Pérez-Sáez, M.J. Tello, in press.
[25] D.L. Wood, K. Nassau, Appl. Opt. 21 (1982) 2978–3298.
[26] J.I. Eldridge, C.M. Spuckler, R.E. Martin, Int. J. Appl. Technol. 3 (2006) 94–104.